

Runoff-driven export of particulate organic carbon from soil in temperate forested uplands

Joanne C. Smith¹, Albert Galy¹, Niels Hovius^{1,2}, Andrew M. Tye³, Jens M. Turowski⁴, Patrick Schleppi⁴

¹Department of Earth Sciences, University of Cambridge, Cambridge, UK

²Present address: German Research Centre for Geosciences GFZ, Potsdam, Germany

³British Geological Survey, Keyworth, Nottingham, UK

⁴Swiss Federal Research Institute WSL, Birmensdorf, Switzerland

Corresponding author:

J. C. Smith

Department of Earth Sciences, University of Cambridge, Downing Street, Cambridge
CB2 3EQ, UK

jcs74@cam.ac.uk

Phone: +44 (0)1223 333455

Fax (department reception): +44 (0)1223 333450

Abstract

We characterise the sources, pathways and export fluxes of particulate organic carbon (POC) in a headwater catchment in the Swiss Alps, where suspended sediment has a mean organic carbon concentration of $1.45\% \pm 0.06$. By chemically fingerprinting this carbon and its potential sources using carbon and nitrogen elemental and isotopic compositions, we show that it derives from binary mixing between bedrock and modern biomass with a soil-like composition. The hillslope and channel are strongly coupled, allowing runoff to deliver recent organic carbon directly to the stream beyond a moderate discharge threshold. At higher flows, more biomass is mobilized and the fraction of modern carbon in the suspended load reaches 0.70, increased from 0.30 during background conditions. Significant amounts of non-fossil organic carbon are thus transferred from the hillslope without the need for extreme events such as landsliding. Precipitation is key: as soon as the rain stops, biomass supply ceases and fossil carbon again dominates. We use rating curves modeled using samples from five storm events integrated over 29-year discharge records to calculate long-term export fluxes of total POC and non-fossil POC from the catchment of 23.3 ± 5.8 and 14.0 ± 4.4 tonnes $\text{km}^{-2} \text{yr}^{-1}$ respectively. These yields are comparable to those from active mountain belts, yet the processes responsible are much more widely applicable. Such settings have the potential to play a significant role in the global drawdown of carbon dioxide via riverine biomass erosion, and their contribution to the global flux of POC to the ocean may be more important than previously thought.

Keywords

Organic carbon, stable isotope geochemistry, carbon export, mountain rivers, runoff processes

1 **1. Introduction**¹

2

3 Export and deep marine burial of carbon from plants and soils, recently fixed from the
4 atmosphere by photosynthesis, transfers carbon from the atmosphere into geological
5 storage (e.g. Berner, 1982; France-Lanord and Derry, 1997). Previous work on
6 carbon export from catchments has focused on active mountain belts because of their
7 importance in the physical erosion budget (Milliman and Syvitski, 1992). For
8 example, recent studies (Carey et al., 2005; Hilton et al., 2008a, 2008b; Lyons et al.,
9 2002) suggest that storm-driven erosion of terrestrial biomass can effectively
10 sequester carbon in tectonically and climatically extreme regimes, such as the active
11 mountain belts of Taiwan and New Zealand. Deep-seated landslides and gully
12 erosion are important in mobilising particulate organic carbon (POC) in extreme
13 events in these environments (Hilton et al., 2008a; West et al., 2011). This POC
14 consists of both modern POC from biomass and fossil POC from sedimentary
15 bedrock. However, there are also indications that erosion processes associated with
16 less intense runoff, driven directly by precipitation, may also be important,
17 particularly in shifting the balance of POC carried in the suspended load towards non-
18 fossil sources (Gomez et al., 2010; Hilton et al., 2012a, 2008b). While deep
19 landslides and gully erosion mobilize bedrock as well as POC, runoff erosion via

¹ Abbreviations used throughout the article:

POC: particulate organic carbon

tPOC: total particulate organic carbon

fPOC: fossil particulate organic carbon

nfPOC: non-fossil particulate organic carbon

C_{org}: organic carbon concentration

SS: suspended sediment

SSC: suspended sediment concentration

TSL: total suspended load

F_{nf}: modeled fraction of non-fossil organic carbon

F_{mod}: fraction of non-fossil organic carbon obtained from radiocarbon measurements

Q_e: effective discharge

20 overland flow removes only the surface layer of soil (Horton, 1945). If such
21 processes are significant, the harvest of non-fossil POC stored in plants and soils
22 could happen anywhere that there is enough rain on vegetated hillslopes to generate
23 overland flow or shallow landslides.

24

25 Evidence for terrestrial POC export in temperate settings unaffected by rapid uplift
26 and tropical storms exists in marine sediments (Gordon and Goñi, 2003; Prahl et al.,
27 1994) and in inputs to the ocean (Hatten et al., 2012), but there is still insufficient
28 understanding of the processes which mobilize POC in the headwater source areas of
29 these deposits. Here, we investigate POC sources and initial pathways under
30 changing hydrologic conditions in a temperate, partly forested headwater catchment in
31 the Swiss Prealps, where the runoff effect is not normally masked by deep-seated
32 landsliding. We find strong evidence for runoff-driven transfer of significant amounts
33 of modern soil-derived biomass during moderate hydrologic conditions, with the
34 proportion of modern carbon in the suspended load increasing with discharge.

35

36 **2. Study Site**

37

38 The Erlenbach is a first order tributary of the Alp River, located 40 km south of
39 Zurich near the town of Einsiedeln. It has a small catchment area (0.74 km^3),
40 elevation 1110 to 1655 m above sea level and average slope of 20% (Hagedorn et al.,
41 2000). The mean annual air temperature is $6 \text{ }^\circ\text{C}$ and mean annual precipitation is
42 2300 mm (Hagedorn et al., 2001), 800 mm of this falling as snow in winter (Schleppi
43 et al., 2005). The largest precipitation events occur as convective rainfall during the
44 summer. In common with other small mountain river systems (Wheatcroft et al.,

45 2010), discharge rises quickly during storms and is highly episodic in response to
46 rainfall (Schleppi et al., 2006).

47

48 The catchment is developed on pelitic turbidites of the Eocene Wägital-Flysch
49 Formation (Winkler et al., 1985). Recent glacial till overlies these rocks, particularly
50 at lower elevations with a cover of up to several metres thick on the lower left bank.
51 Both bedrock and drift are fine-grained, clay-rich and impermeable, resulting in
52 water-saturated gleysols. Creep landslides are common, particularly in the lower
53 reaches where steep channel sides cut into active complexes developed mainly in the
54 till. These incrementally deliver substantial amounts of sediment to the stream
55 channel during winter, which is removed by summer storms (Schuerch et al., 2006).
56 The Erlenbach lacks a well-developed riparian zone and has a step-pool morphology
57 with both logs and boulders forming the steps (Turowski et al., 2009). The catchment
58 is 40% forest and 60% wetland and alpine meadow (Turowski et al., 2009). The main
59 tree species are Norway Spruce (*Picea abies*) and European Silver Fir (*Abies alba*),
60 with some green Alder (*Alnus viridis*) (Schleppi et al., 1999).

61

62 The Erlenbach is an experimental catchment of the Swiss Federal Institute for Forest,
63 Snow and Landscape Research (WSL) (Hegg et al., 2006). Over the time period
64 1983-2011 inclusive, discharge (Q) recorded at 10-minute intervals ranged from 0 to
65 11946 l s^{-1} with an average (Q_{mean}) of 38.6 l s^{-1} . In this study, we report discharges
66 relative to this value (as Q/Q_{mean}), as well as absolute values, to allow comparison to
67 other catchments. Over the monitoring period, flow was less than or equal to Q_{mean}
68 for 77% of the time, with such discharges accounting for about 1% of suspended
69 sediment transport. Less than 1% of discharges were above the threshold at which

70 substantial bedload transport starts, which corresponds to $Q/Q_{\text{mean}} \sim 13$ (Turowski et
71 al., 2011). The catchment is also a site for the NITREX project (NITROgen saturation
72 EXperiments) (Wright and Rasmussen, 1998), and has three <1 ha sub-plots equipped
73 with V-notch weirs in forest, forest with experimental nitrogen addition, and meadow
74 (Schleppi et al., 1998).

75

76 **3. Methods**

77

78 POC in riverine suspended sediment is a mixture of carbon from two or more end
79 member sources (Blair et al., 2003; Hilton et al., 2008a, 2008b; Komada et al., 2004;
80 Leithold et al., 2006). It is particularly important to distinguish between carbon from
81 fossil and non-fossil sources, because re-burial of fossil carbon has no effect on
82 contemporary CO_2 drawdown, while burial of non-fossil carbon bypasses the usual
83 rapid oxidation pathway and sequesters carbon (Berner, 1982). Mixing relationships
84 can be primarily elucidated in $\text{N/C}-\delta^{13}\text{C}$ and $\text{C/N}-\delta^{15}\text{N}$ space (e.g. Hilton et al., 2010),
85 while ^{14}C provides an additional constraint on the input of fossil carbon (e.g. Blair et
86 al., 2003; Hilton et al., 2008b; Komada et al., 2005).

87

88 *3.1 Sample Collection*

89

90 Instantaneous suspended sediment samples were collected direct from the stream at
91 the upper gauging station in 100 ml plastic bottles, every few minutes during five
92 storm events in July 2010. The largest of these (12 July) had a return period of about
93 one year and a peak discharge of 2290 l s^{-1} , corresponding to a Q/Q_{mean} of ~ 59 . The
94 remaining four events took place within 10 days and covered a range of peak

95 discharges from 300 to 1580 l s⁻¹ [Table 1]. With the exception of the 12 July event,
96 the storms were characterised by intermittent rain. The hydrographs for three of the
97 events are shown in Figure 1. After collection, each turbid sample was passed
98 through a 0.2 µm nylon filter within two weeks (mostly within three days), following
99 interim storage at 5 °C. The filters with sediment were stored in glass petri dishes at -
100 18 °C before lyophilization.

101

102 110 samples from potential sources for the riverine suspended sediment, including
103 bedrock, surface soil, deeper soil profiles, foliage, wood, bedload and material from
104 landslides and banks adjoining the channel, were collected between October 2009 and
105 August 2010. All samples were stored in sealed plastic bags and oven-dried in
106 covered foil dishes at <80 °C as soon as possible (1-12 days) after collection.

107

108 Surface soil and foliage were collected in transects across the catchment at a range of
109 elevations, covering all major geomorphologic and ecologic conditions. At each
110 locality, samples as representative as possible of the immediate surroundings were
111 taken. Surface soil (a combination of O and A layers) was collected from the top ~10
112 cm with a clean trowel, after removal of overlying vegetation. Although the timing of
113 collection could potentially affect the isotopic composition of soil samples because
114 more decomposed litter could be enriched in ¹³C and ¹⁵N (e.g. Dijkstra et al., 2008),
115 the collection method and subsequent processing result in samples homogenised over
116 a long enough period to negate any seasonal differences. Foliage included multiple
117 samples, comprising needles, leaves and twigs from all sides, of the three main tree
118 types and representative understory. Samples of woody debris embedded in
119 landslides and the channel bed were also collected across the catchment. Throughout

120 this study, 'foliage' and 'wood' are used as convenient terms for different types of
121 standing biomass, and include all associated microbial organisms.

122

123 Two vertical profiles were taken through landslides (down to 80 cm and 170 cm), and
124 two through stable hillslopes (to 60 cm and 160 cm); these were sampled at 10-60 cm
125 intervals. In reporting the results, the uppermost soil samples from each stable
126 hillslope profile are treated as 'surface soils' and are excluded from the profile group
127 ('deep soils'). Soil is generally poorly developed on top of the landslides and so no
128 such distinction is made. 22 bedrock samples were obtained across the catchment
129 (from both hillslopes and stream bed). Bedload was collected along the full length of
130 the main channel.

131

132 Discharge-proportional compound samples of suspended sediment were collected
133 from the forest control and meadow sub-plots weekly (when there was enough runoff)
134 between August 2009 and August 2011. A representative subset of each of these was
135 analyzed to obtain an estimate of the hillslope input signal.

136

137 *3.2 Sample Preparation*

138

139 For source sediments, only the suspendable fraction (<2 mm), isolated through wet-
140 and dry-sieving, was subjected to further analysis. Suspended sediment occasionally
141 contained material >2 mm; these particles, mainly large organic material such as
142 spruce or fir needles, were excluded from chemical analysis, though their weight was
143 recorded and used in calculations of suspended sediment concentrations. Bedrock and
144 vegetation samples were analyzed in bulk.

145

146 All samples were homogenized using either a ball mill grinder, a pestle and mortar
147 (for small samples) or a blade mill grinder (for vegetation). Bedrock samples were
148 first crushed using a jaw crusher to fragments <5 mm. Pulverized samples and blanks
149 were heated to 80 °C with dilute (1M) hydrochloric acid for three hours to remove
150 carbonate, rinsed with de-ionized water and dried thoroughly (France-Lanord and
151 Derry, 1994; Galy et al., 2007a; Hilton et al., 2008a). Between 5 and 30% of each
152 sample was lost through the carbonate removal process, with no apparent disparity
153 between different types of material. Most of this loss corresponds to carbonate
154 dissolution plus loss of particles on the vessels used in treatment (Galy et al., 2007a;
155 Hilton et al., 2008a; Brodie et al., 2011). This process unavoidably causes loss of a
156 labile fraction of organic C, and the results reported here relate to the non-labile
157 fraction only. However, it is this more recalcitrant fraction that is most likely to be
158 ultimately buried in the ocean, and therefore of interest in this study. This procedure
159 was carried out on all samples (including vegetation), so that any isotopic
160 fractionation effects of the de-carbonation process (Brodie et al., 2011) are universally
161 applied and the results are internally consistent.

162

163 *3.3 Analysis*

164

165 Processed, powdered samples were combusted, and the resultant N₂ and CO₂
166 concentrations (reported in weight %) and carbon and nitrogen isotopic compositions
167 ($\delta^{13}\text{C}$ and $\delta^{15}\text{N}$, reported in ‰) were obtained using a flash Elemental Analyser
168 coupled to a continuous flow Nier-type mass spectrometer via a gas bench for gas
169 separation. All measurements were corrected for procedural blanks following

170 published methods (Hilton et al., 2010; 2012b). Multiple aliquots of varying material
171 were analyzed; the average relative difference was $\ll 0.001\%$ for C and N, and
172 average standard deviation was 0.05‰ for $\delta^{13}\text{C}$ and 0.3‰ for $\delta^{15}\text{N}$. To test for long-
173 term machine drift, 10 samples were analyzed a second time one year after the first
174 analysis. This set of repeats had an average relative difference of 0.06% for C and
175 0.07% for N, and average standard deviation of 0.05‰ for $\delta^{13}\text{C}$ and 0.3‰ for $\delta^{15}\text{N}$.
176
177 ^{14}C measurements on 14 graphitized samples were obtained by accelerator mass
178 spectrometry at the NERC Radiocarbon Laboratory in East Kilbride, UK. Reported
179 results comprise the proportion of ^{14}C atoms in each sample compared to that present
180 in the year 1950 (F_{mod}), $\Delta^{14}\text{C}$ in ‰ , and conventional radiocarbon age. The standard
181 IAEA-C5, subjected to the same carbonate-removal procedure as the samples,
182 returned ^{14}C to within 1σ of the consensus value.

183

184 **4. Results**

185

186 *4.1 Concentration and Composition of Organic Carbon in Source Materials*

187

188 Composition data for riverine suspended sediment, hillslope runoff input and major
189 carbon stores within the catchment are summarised in Table 2 while the radiocarbon
190 data are shown separately in Table 3.

191

192 Bedrock has organic carbon concentrations (C_{org}) ranging from $0.16\text{--}1.15\%$, with a
193 mean of $0.54\% \pm 0.11$ ($\pm 2\sigma_{\text{mean}}$, $n = 22$), C/N of 7.81 ± 1.7 , $\delta^{13}\text{C} = -25.71\text{‰} \pm 0.36$
194 and $\delta^{15}\text{N} = 3.34\text{‰} \pm 0.26$. Bedload, channel banks and landslide deposits have

195 similarly low C_{org} (all means $<1\%$), and are compositionally very similar to bedrock.
196 Modern sources, surface soil ($n = 17$) and foliage ($n = 8$), have significantly higher
197 C_{org} ($16.5\% \pm 6.3$ and $46.9\% \pm 2.0$ respectively). Both pools have high C/N and are
198 depleted in heavy isotopes of C and N, but do not overlap: surface soil has C/N of
199 17.9 ± 2.2 , $\delta^{13}\text{C}$ of $-26.84\text{‰} \pm 0.48$ and $\delta^{15}\text{N}$ of $-1.33\text{‰} \pm 0.76$, while foliage has C/N
200 of 55.5 ± 17 , $\delta^{13}\text{C}$ of $-28.30\text{‰} \pm 1.13$ and $\delta^{15}\text{N}$ of $-5.87\text{‰} \pm 1.67$. The ^{14}C results
201 from surface soils show that they are essentially modern; the one soil F_{mod} value of
202 less than 1 is explained by its close association with a landslide and lack of overhead
203 forest canopy. Woody debris (up to 4000 years old) have high C_{org} ($49.1\% \pm 1.8$; $n =$
204 12), high C/N (173 ± 98), are depleted in ^{15}N ($\delta^{15}\text{N} = -3.99\text{‰} \pm 1.29$), and enriched in
205 ^{13}C ($\delta^{13}\text{C} = -25.25\text{‰} \pm 0.69$), in contrast to modern vegetation.

206

207 Landslide complexes have homogeneous compositions throughout their depth, with
208 no systematic variations in C_{org} , C/N, $\delta^{13}\text{C}$ or $\delta^{15}\text{N}$. In contrast, the soil profiles from
209 stable slopes show a significant decrease in C_{org} and C/N (to levels comparable to the
210 landslides) at ~ 40 -60 cm depth, although there are no clear patterns in isotopic
211 composition. The landslide profiles sampled show very little incorporation of non-
212 fossil material, while the soil profiles (even without the uppermost samples) document
213 a transition from surface-like horizons to a more fossil-like layer at depth.

214

215 *4.2 Concentration of Organic Carbon in Riverine Suspended Sediment*

216

217 The observed range of C_{org} in riverine suspended sediment samples was 0.78-2.52%,
218 with a mean of $1.45\% \pm 0.06$ ($\pm 2\sigma_{\text{mean}}$, $n = 122$). Within each event, there appears to
219 be no consistent pattern in C_{org} over the hydrograph [Figure 1]. However, when all

220 data are considered together, there is a clear parabolic pattern in the variation of C_{org}
221 with both Q and suspended sediment concentration (SSC), with negligible difference
222 in C_{org} patterns between rising and falling limbs. The product of Q and SSC combines
223 both effects in the parameter 'total suspended load' (TSL, in $g\ s^{-1}$) [Figure 2]. At low
224 TSL, C_{org} is initially variable, then decreases with increasing TSL. Beyond a
225 threshold of $\sim 500\ g\ s^{-1}$ (corresponding to $Q/Q_{mean} \sim 10$ and $SSC \sim 1600\ mg\ l^{-1}$), C_{org}
226 increases: this trend continues up to at least $\sim 40000\ g\ s^{-1}$ ($Q/Q_{mean} \sim 60$). The
227 threshold is reached under moderate conditions, occurring several times per year, and
228 in four of the five events sampled. Because of this change in behaviour, we take
229 flows of $Q/Q_{mean} < 10$ to represent background conditions, after Gomez et al. (2010).

230

231 *4.3 Composition of Organic Carbon in River and Runoff Suspended Sediment*

232

233 C/N ranges from 6.9 to 13, with a mean of 9.55 ± 0.24 ($\pm 2\sigma_{mean}$, $n = 122$); $\delta^{13}C$ ranges
234 from -27.55 to -24.25% with a mean of $-26.33\% \pm 0.08$; and $\delta^{15}N$ ranges from 0.15
235 to 5.08% with a mean of $2.21\% \pm 0.16$. There are compositional differences between
236 samples collected on the rising and falling limbs, and during rain and dry periods
237 [Table 2], with the former group having higher C/N and lower $\delta^{13}C$ and $\delta^{15}N$ in each
238 case. The mean F_{mod} for the six suspended sediment samples sent for $\Delta^{14}C$ analysis
239 was 0.65 ± 0.08 ($\pm 2\sigma_{mean}$, $n = 6$). In both N/C- $\delta^{13}C$ and C/N- $\delta^{15}N$ compositional space
240 where mixing relationships are linear, POC in riverine suspended sediment samples
241 plots in a broadly linear range bounded approximately by bedrock and soil [Figure 3].
242 Suspended sediment samples with higher $\delta^{15}N$ than the bedrock range may indicate
243 that the stream is sampling bedrock compositions not exposed at the surface
244 elsewhere in the catchment.

245

246 In contrast to most pools, the mean composition of carbon in the hillslope runoff
247 suspended sediment samples suggests different relationships in the N/C- $\delta^{13}\text{C}$ and
248 C/N- $\delta^{15}\text{N}$ plots. In N/C- $\delta^{13}\text{C}$ space, forest and meadow runoff samples have the same
249 composition within error, and lie at the low-N/C, low- $\delta^{13}\text{C}$ end of the riverine
250 suspended sediment range. In C/N- $\delta^{15}\text{N}$ space, forest and meadow runoff are
251 compositionally distinct, and both lie outside the compositional range of riverine
252 suspended sediment [Figure 3]. Both sets of runoff samples have higher C_{org} values
253 than riverine suspended sediment, of $9.12\% \pm 0.9$ ($\pm 2\sigma_{\text{mean}}$, $n = 38$; forest) and 15.9%
254 ± 1.7 ($\pm 2\sigma_{\text{mean}}$, $n = 10$; meadow).

255

256 **5. Discussion**

257

258 Both the compositional distribution and F_{mod} values of riverine suspended sediment
259 are consistent with mixing between fossil and non-fossil end members. Although C_{org}
260 in the suspended sediment is always higher than that of bedrock, indicating that there
261 is some non-fossil input at all times, this input becomes increasingly significant at
262 higher TSL and Q [Figure 4]. POC from samples collected at low TSL cover the
263 whole compositional range, but are strongly concentrated towards low C/N and high
264 $\delta^{13}\text{C}$ and $\delta^{15}\text{N}$ (that is, a ‘fossil’ composition). During larger events, there is a bulk
265 shift away from the fossil towards the non-fossil end of the mixing line.

266

267 *5.1 Nature of the Non-Fossil End Member*

268

269 Because the composition of the POC exported from the catchment plots in the space
270 between several different carbon pools, careful definition of the end members is
271 necessary. Although the ‘fossil’ chemical composition of bedload, landslides and
272 channel banks suggests that these pools all derive from bedrock, we take bedrock
273 alone as the unequivocal fossil end member. Of the non-fossil carbon pools, surface
274 soil and foliage are closest to but not exactly on the mixing trend defined by bedrock
275 and the suspended sediment samples. Non-fossil material comes from a range of
276 sources, so we calculate a hypothetical non-fossil end member using F_{mod} and $\delta^{13}\text{C}$
277 following the procedure defined by Hilton et al. (2010). Briefly, the $\delta^{13}\text{C}$ of the
278 individual non-fossil end member for each suspended sediment sample with known
279 F_{mod} is calculated according to the mixing relationship

$$280 \quad \delta^{13}\text{C}_{\text{sample}} = F_{\text{mod}} \cdot \delta^{13}\text{C}_{\text{nf}} + (1 - F_{\text{mod}}) \cdot \delta^{13}\text{C}_{\text{fos}}$$

281 where $\delta^{13}\text{C}_{\text{nf}}$ and $\delta^{13}\text{C}_{\text{fos}}$ are the $\delta^{13}\text{C}$ values of a hypothetical non-fossil end member
282 and the average $\delta^{13}\text{C}$ of bedrock samples respectively. The mean of the six calculated
283 values of $\delta^{13}\text{C}_{\text{nf}}$ is taken. We then use lines of best fit, calculated using only points
284 with $Q/Q_{\text{mean}} > 10$, to find the corresponding N/C, C/N and $\delta^{15}\text{N}$. Uncertainties of
285 twice the standard error on the mean of the initial $\delta^{13}\text{C}$ value are propagated through
286 this calculation procedure. The resulting hypothetical end member [Figure 4] has C/N
287 of 15.8 ± 6.8 , $\delta^{13}\text{C}$ of $-27.15\text{‰} \pm 0.53$ and $\delta^{15}\text{N}$ of $0.61\text{‰} \pm 1.40$. This is much more
288 similar to surface soil than foliage, suggesting that soil is heavily implicated in the
289 non-fossil POC input. It is also similar to the forest hillslope runoff signal in N/C-
290 $\delta^{13}\text{C}$ space, but the two have distinctly different $\delta^{15}\text{N}$ values.

291

292 The concentrations of fossil and non-fossil POC in milligrams per litre can be
293 obtained for each sample, and then used to determine independent relationships with

294 discharge, if we know the proportion of organic carbon derived from non-fossil
295 sources. Given the simple mixing exhibited by the system, it is possible to model this
296 parameter for each suspended sediment sample, denoted F_{nf} to distinguish it from F_{mod}
297 measured using ^{14}C , using the mixing equation given above, the $\delta^{13}\text{C}$ of the sample
298 and two end members (Hilton et al., 2010). We used bedrock and the hypothetical
299 non-fossil end member determined above. Owing to scatter in the system, calculated
300 F_{nf} values for 9% of the samples fell outside the possible range of 0-1.1. For these, a
301 value of 0 or 1.1 was substituted as appropriate. On the samples sent for ^{14}C analysis,
302 F_{nf} shows reasonable agreement with F_{mod} , reproducing it to within 0.24 at the 95%
303 level.

304

305 *5.2 Long-Term Carbon Export Flux: Fossil and Non-Fossil Components*

306

307 It is important to consider not only the export of total carbon, but of fossil carbon and
308 non-fossil carbon separately, because only non-fossil carbon burial has an effect on
309 contemporary carbon dioxide drawdown (e.g. Berner, 1982; Blair and Aller, 2012).
310 Because distinct pools of organic carbon behave differently, shown by the changing
311 composition of POC at different discharges, their long-term export should be
312 considered independently (Wheatcroft et al., 2010).

313

314 We used the calculated F_{nf} values to construct rating curves describing the
315 relationships between discharge and load of four components: suspended sediment
316 (SS), total POC (tPOC), fossil POC (fPOC) and non-fossil POC (nfPOC). These are
317 all power laws of the form $a(Q/Q_{mean})^b$ [Table 4; Figure 5]. Because of the threshold
318 switch to POC addition at $Q/Q_{mean} > 10$, and the fact that flows above background

319 conditions are disproportionately important in transporting sediment and POC, we
320 would ideally only use samples at $Q/Q_{\text{mean}} > 10$ to fit the rating curves. However, this
321 is mathematically unsatisfactory as it restricts the range of Q/Q_{mean} to less than one
322 order of magnitude and results in large uncertainties on a and b . We therefore use
323 relationships determined using the full sample set (three orders of magnitude in
324 Q/Q_{mean}), but check their geomorphological validity by comparing with those
325 determined using only samples with $Q/Q_{\text{mean}} > 10$, finding in all cases that a and b are
326 well within error [Table 4].

327

328 The larger exponent for tPOC ($b = 1.33$) compared to SS ($b = 1.19$) means that
329 relatively more POC is exported at higher discharges than SS, in contrast to the
330 relationships seen in the Waipaoa River (New Zealand) and Alsea River (Oregon)
331 (Wheatcroft et al., 2010). The effect is even more pronounced for nfPOC ($b = 1.45$)
332 than for tPOC. The exponent for fPOC ($b = 1.08$) is within error of that for SS,
333 reflecting their shared clastic origin. Differences in the rating curve exponents are
334 mirrored by those in effective discharge (Q_e), the discharge that, on average,
335 transports the largest proportion of a given constituent load (Andrews, 1980; Nash,
336 1994; Wheatcroft et al., 2010). Q_e is greatest for nfPOC (corresponding to Q/Q_{mean} of
337 13.4), and lowest for fPOC (5.6). Q_e for all four components [Table 4] corresponds to
338 similar flows (relative to Q_{mean}) to many other small mountain rivers (Wheatcroft et
339 al., 2010).

340

341 Applying these rating relationships to the discharge record for the Erlenbach, we
342 modeled the export of the four components over the period 1983-2011 inclusive, with
343 full results shown in [Table 5]. The mean annual yields and export fluxes of each

344 component were: $1220 \pm 232 \text{ t yr}^{-1}$ and $1648 \pm 313 \text{ t km}^{-2} \text{ yr}^{-1}$ (SS); $17.3 \pm 4.3 \text{ t yr}^{-1}$
345 and $23.3 \pm 5.8 \text{ t km}^{-2} \text{ yr}^{-1}$ (tPOC); $7.4 \pm 1.2 \text{ t yr}^{-1}$ and $10.1 \pm 1.6 \text{ t km}^{-2} \text{ yr}^{-1}$ (fPOC);
346 and $10.4 \pm 3.2 \text{ t yr}^{-1}$ and $14.0 \pm 4.4 \text{ t km}^{-2} \text{ yr}^{-1}$ (nfPOC). These amounts of fossil and
347 non-fossil carbon exported were used to calculate a mean F_{nf} value for each year, both
348 overall and at different discharges [Table 5]. According to the model, 61% of all the
349 organic carbon exported from the Erlenbach over this 29-year period came from non-
350 fossil sources (mean overall $F_{\text{nf}} = 0.61 \pm 0.02$).

351

352 The yield of fPOC based on rating curve [Table 5] is within error of the ‘expected’
353 mean annual yield of fossil carbon ($7.3 \pm 1.3 \text{ t yr}^{-1}$), reached by multiplying the
354 average C_{org} of the bedrock samples by suspended sediment yield. This suggests that
355 there is no significant remineralization of fossil organic carbon during bedrock
356 erosion and export from these headwaters, in common with findings from the French
357 Alpes-de-Haute-Provence (Graz et al., 2011), although oxidation may occur during
358 onward transport and floodplain storage (Bouchez et al., 2010).

359

360 The effect of the different rating curve exponents is illustrated by comparing the
361 proportional yields of each component at different discharges, with the largest flows
362 transporting a greater proportion of nfPOC than tPOC, and a greater proportion of
363 tPOC than SS and fPOC. We define three discharge class boundaries, corresponding
364 to $Q/Q_{\text{mean}} = 1, 10$ and 60 . $Q/Q_{\text{mean}} = 10$ is the threshold above which POC is added,
365 while $Q/Q_{\text{mean}} = 60$ is the approximate limit of discharges we have sampled. This
366 limit is only exceeded very rarely (5.4×10^{-5} of the time), but can be exceeded
367 substantially: the largest discharge recorded in the 10-minute dataset during the
368 monitoring period was 11950 l s^{-1} ($Q/Q_{\text{mean}} \sim 309$), on 25 July 1984. Our results show

369 that the lowest discharge class (the state of the stream for over three quarters of the
370 time) is insignificant in terms of both SS and POC export and POC would be
371 dominated by fossil origin (modeled $F_{nf}=0.30$). Conversely, if the same rating curve
372 applied above the upper limit, discharges of $Q/Q_{mean} > 60$ would transport considerable
373 quantities of sediment, POC and particularly nfPOC (10, 12 and 13% of total transport
374 respectively), despite occurring less than 0.01% of the time. Beyond $Q/Q_{mean} = 60$, F_{nf}
375 would be 0.76 if the same rating relationship applied. However, because of the lack
376 of constraints on processes or suspended load at these flows, this assumption is not
377 conservative; for example, if landslides are activated, there may be an increase in the
378 proportion of fPOC. Instead, we assume a constant load of all four components for
379 $Q/Q_{mean} > 60$, giving F_{nf} of 0.70 for this discharge range, and conservative estimate for
380 the total yields.

381

382 *5.3 Sources and Pathways of Non-fossil Organic Carbon in the Erlenbach*

383

384 In order to draw more general conclusions from the detailed study of nfPOC export in
385 the Erlenbach, the origins and harvesting mechanism of this nfPOC need to be better
386 understood. When there is a small overall load, incidental, local mobilisation
387 dominates and suspended sediment shows the natural variability of catchment
388 composition and process [Figures 2 and 4]. Subsequent POC dilution to a minimum
389 of ~1% [Figure 2] must be due to an increased input of material with low C_{org} , by a
390 mechanism that does not require high-energy flows. This is likely due to higher
391 discharge causing an increase in bed shear stress, which mobilizes fossil-derived
392 material already in the channel. This lithic material (left by previous events, delivered
393 to the channel by creep landslides, or exposed bedrock) contains small amounts of

394 fossil C_{org} : bedrock, bedload, landslide and channel bank pools all have average C_{org}
395 <1%.
396
397 Beyond the 500 g s^{-1} threshold (at $Q/Q_{mean} \sim 10$), material with a higher C_{org} than
398 bedrock or any of the groups derived from it must be added to the suspended load.
399 Addition of fossil organic carbon released from bedrock, either directly or via
400 landslides and channel banks, cannot explain the compositional trends observed in the
401 suspended load with increasing discharge [Figures 3 and 4]. Instead, the sourcing
402 mechanism must mobilize only surface soil, litter and vegetation, in a way that gives
403 the composition of the non-fossil end member calculated above. This strongly
404 suggests that surface runoff processes are responsible, but there is a compositional
405 discrepancy in $\delta^{15}\text{N}$ between runoff suspended sediment and the hypothetical end
406 member. However, the subplots (where the runoff suspended sediment samples were
407 collected) are situated towards the edge of the catchment, whereas runoff entering the
408 stream comes from lower, steeper hillslopes. Here, the bed stress is higher and runoff
409 may penetrate deeper via transient gullying (Horton, 1945), allowing overland flow to
410 pick up more soil and reducing $\delta^{15}\text{N}$ values to the hypothetical composition.
411 Considering these processes, hillslope activation driven by surface runoff can account
412 for the change in composition of river suspended sediment POC above background
413 flow, and so for the material added in this hydrological phase. This is supported by
414 end member mixing analysis using dissolved nutrient tracers in the Erlenbach
415 catchment which suggests that, at moderate summer storm peak discharges, over half
416 the runoff in the stream comes directly from precipitation (Hagedorn et al., 2000).
417 The $Q/Q_{mean} = 10$ threshold, therefore, appears to reflect a critical shear stress at
418 which slope material is mobilised.

419

420 The flood hydrographs [Figure 1] suggest that as soon as discharge has peaked,
421 hillslopes are deactivated and delivery of non-fossil organic carbon to the stream is
422 stanchied, shown by decrease in C/N and $\delta^{13}\text{C}$. This reflects the differing
423 compositions of suspended sediment collected during the rising limb of the
424 hydrograph, when it is usually raining, and falling limb, when it is largely dry.
425 Similarly, the F_{nf} value is significantly higher for samples collected during rainfall
426 (0.54 ± 0.05 ; $\pm 2\sigma_{\text{mean}}$, $n = 85$) and the rising limb (0.51 ± 0.05 ; $n = 72$) than dry
427 periods (0.25 ± 0.06 ; $n = 37$) or the falling limb (0.36 ± 0.08 ; $n = 50$).

428

429 *5.4 Caveats*

430

431 So far we have only considered processes operating during moderate to large flows:
432 having only sampled up to $Q/Q_{\text{mean}} \sim 60$, we have no insight into the geomorphic
433 dynamic at very high flow rates. If extreme precipitation could trigger rapid
434 landslides, then the system may cross a threshold into a more ‘active margin-like’
435 mode of behaviour, where mass wasting during storms causes progressive dilution of
436 modern organic carbon (Blair and Aller, 2012; Kao and Liu, 1996; Masiello and
437 Druffel, 2001).

438

439 The calculated F_{nf} of POC exported from the catchment is systematically biased by
440 not including bedload, because bedload is closely related to bedrock [Figure 3] and
441 contains dominantly fossil carbon. This is particularly true in small catchments with
442 high sediment load like the Erlenbach, where bedload is relatively more important
443 than in large mountain rivers (Rickenmann et al., 2012). We chose to exclude

444 bedload in order to enable comparison with other sites, since only suspended load data
445 are available at most locations. However, because bedload transport is constrained to
446 some extent in the Erlenbach, we briefly discuss the implications. The total sediment
447 volume accumulated in the retention basin between August 1982 and October 2012
448 was 17730 m³, including pore space and suspendable fines. Using a bulk density of
449 1750 kg m⁻³ (Rickenmann and McArdell, 2007), and assuming that 75-80% of the
450 material is larger than 2 mm, this gives ~800 tonnes per year. Using the bedrock C_{org}
451 of 0.54%, this equates to an additional ~4 tonnes of organic carbon per year. An
452 alternative estimate, assuming that bedload volume is approximately equal to
453 suspended load volume in the Erlenbach (Turowski et al., 2010), gives an additional
454 ~7 tonnes of organic carbon per year. These figures suggest that, if bedload as well as
455 suspended load is considered, the overall F_{nf} would decrease from 0.6 [Table 5] to
456 between 0.4 and 0.5. A further consideration is the possibility that non-fossil carbon
457 in the form of coarse woody debris is transported in the bedload, meaning that total
458 nfPOC export is also underestimated by our analysis. However, more work is needed
459 to quantify this.

460

461 Additional biases may result from the fact that our rating curves and flux estimates are
462 based on samples collected during the summer only and so take no account of
463 possible seasonal changes in the relationships between discharge and tPOC, fPOC and
464 nfPOC concentrations. It is likely that significantly different processes to those we
465 have constrained occur only during the winter and early spring, when there is snow on
466 the ground or melting. The last panel in Figure 1 shows that, although discharge is
467 highest during snow melt in April-May, suspended sediment concentrations are
468 relatively low throughout winter and spring. Multiplying mean discharge by mean

469 SSC gives mean total suspended load values of $\sim 3 \text{ g s}^{-1}$ for winter/spring (December-
470 May) and $\sim 15 \text{ g s}^{-1}$ for summer/autumn (June-November). Thus, the mass of material
471 exported under the conditions we have constrained is approximately five times greater
472 than that exported at other times. Even if somewhat different processes were shown
473 to operate in winter and taken into account, the long-term fluxes would not change
474 substantially and our conclusions would be unaffected.

475

476 *5.5 Global Significance of POC Flux and Processes Observed in the Erlenbach*

477

478 The rate of export of non-fossil POC from the Erlenbach ($14.0 \pm 4.4 \text{ tonnes km}^{-2} \text{ yr}^{-1}$)
479 is broadly comparable to yields of non-fossil POC reported from Taiwan (21 ± 10
480 $\text{tonnes km}^{-2} \text{ yr}^{-1}$) (Hilton et al., 2012a) and New Zealand ($\sim 39 \text{ tonnes km}^{-2} \text{ yr}^{-1}$)
481 (Hilton et al., 2008a), and an order of magnitude greater than from the Ganges-
482 Brahmaputra basin ($\sim 3 \text{ tonnes km}^{-2} \text{ yr}^{-1}$) (Galy et al., 2007b). However, the real
483 significance lies in the contrasting processes responsible for these fluxes and their
484 geographical scope. In some mountainous settings, high rates of tectonic uplift, often
485 combined with intense cyclonic storms, drive deep-seated landsliding and flooding on
486 a scale and frequency not seen elsewhere. In contrast, runoff-driven hillslope
487 activation observed in the Erlenbach are widely applicable and do not require
488 catastrophic events to initiate significant carbon POC export. Similar processes are
489 likely to occur wherever there is rain on steep, soil-mantled hillslopes that are
490 effectively coupled to stream channels so that there is a direct, unfiltered transfer of
491 material into them.

492

493 Meybeck (1993) estimated that 18% of total atmospheric (i.e. modern) carbon (overall
494 flux of $542 \times 10^{12} \text{ g yr}^{-1}$) is exported as soil-derived POC, or $\sim 98 \times 10^{12} \text{ g yr}^{-1}$. A
495 direct comparison with the Erlenbach non-fossil POC flux of $14 \text{ tonnes km}^{-2} \text{ yr}^{-1}$
496 suggests that $\sim 4.6\%$ of the world's total land area behaving like the Erlenbach could
497 account for this flux. The global area covered by temperate broadleaf and mixed
498 forests is ~ 13.5 million km^2 (Mace et al., 2005), or 9% of the world's land; if other
499 biomes with the potential to host runoff-driven POC export are included (such as
500 temperate coniferous forests and montane grasslands), this rises to 15%. However, it
501 should be noted that steep topography is also an essential ingredient in creating
502 Erlenbach-like conditions. While the biome classification, based on WWF terrestrial
503 ecoregions (Olson et al., 2001), takes account of some factors related to topography,
504 such as climate, it is unlikely to accurately map the topographic limits for the runoff
505 processes described above. Nevertheless, these considerations tentatively suggest that
506 the contribution to global riverine POC flux, particularly the export of non-fossil
507 POC, from Erlenbach-like settings may be more significant than suggested by extant
508 global estimates.

509

510 **6. Conclusions**

511

512 We have characterised the processes responsible for transferring organic carbon from
513 hillslope to stream in an alpine headwater catchment with C_{org} -rich bedrock, a high
514 degree of hillslope-channel coupling and no extreme mass wasting over the timescale
515 of the study. Additionally, we have determined the long-term yields of suspended
516 sediment, total POC, fossil POC and non-fossil POC from this system under moderate
517 conditions.

518

519 Suspended sediment exported from the Erlenbach has a mean C_{org} of 1.45 ± 0.06 %.
520 Both concentration and composition of this organic carbon vary systematically with
521 hydrological conditions, although variations over any single hydrograph are highly
522 individual. At low discharge, POC concentration and composition is highly variable,
523 due to natural heterogeneity in the small amount of material transported. As
524 discharge increases (along with total suspended load), in-channel clearing causes
525 initial dilution of POC. At a moderate, frequently-crossed threshold ($Q/Q_{\text{mean}} = 10$),
526 the hillslope becomes active and runoff delivers additional POC to the stream in the
527 form of largely soil-derived biomass, causing a bulk shift to higher C/N and lower
528 $\delta^{13}\text{C}$ and $\delta^{15}\text{N}$. This is associated with an increase in the F_{nf} from 0.30 during
529 background flow to 0.70 at the highest discharges we have sampled ($Q/Q_{\text{mean}} \sim 60$).
530 Active precipitation is crucial to the mechanism, with riverine suspended sediment
531 showing greater non-fossil influence and significantly higher F_{nf} during rain and on
532 the rising limb than when the rain has stopped and flow is waning. Landslides and
533 channel bank collapse do not regularly contribute to the POC exported under these
534 conditions, but may be activated at extremely high flow rates.

535

536 Rating curves show power law relationships between discharge and four components:
537 suspended sediment, total POC, fossil POC and non-fossil POC. All exponents are
538 >1 , with fossil POC the lowest at 1.08. Total POC has a significantly higher exponent
539 than suspended sediment, and non-fossil POC has one greater still. Over the past 29
540 years, the conservative estimates of average export fluxes of suspended sediment,
541 total POC, fossil POC and non-fossil POC (in tonnes $\text{km}^{-2} \text{yr}^{-1}$) were 1648 ± 313 , 23.3
542 ± 5.8 , 10.1 ± 1.6 and 14.0 ± 4.4 respectively.

543

544 We propose that the runoff-driven export of soil-derived POC observed in the
545 Erlenbach is a model for other temperate forested uplands where there is good
546 connectivity between the hillslope and channel. The yield of non-fossil POC from
547 such settings is of the same order of magnitude as those reported from active margin
548 mountain belts, yet the potential area available for this non-catastrophic mode of POC
549 mobilisation extends to large parts of the Earth's continents. Considering our results
550 in the context of previous global estimates of riverine POC discharge, it seems likely
551 that the collective contribution of settings where these processes operate may be more
552 important than previously thought. If the non-fossil POC exported from the
553 Erlenbach and similar catchments is ultimately buried in the ocean, this mechanism
554 could significantly contribute to carbon dioxide drawdown on geological timescales.

Acknowledgements

This work was completed as part of a PhD studentship funded by NERC, partly via the British Geological Survey's British Universities Funding Initiative (BUFI).

Radiocarbon analysis was supported by NRCF grant number 1573.0911. We thank staff at WSL, the Godwin Institute and the Department of Geography, University of Cambridge, for assistance with field- and lab-work. Two anonymous reviewers gave insightful comments that helped to improve the manuscript, and Mike Ellis provided useful feedback on an earlier version.

References

- Andrews, E. D. (1980). Effective and bankfull discharges of streams in the Yampa River basin, Colorado and Wyoming. *J Hydrol* **46**, 311-330, doi:10.1016/0022-1694(80)90084-0
- Berner, R. A. (1982). Burial of organic carbon and pyrite sulfur in the modern ocean; its geochemical and environmental significance. *Am J Sci* **282**, 451-473, doi:10.2475/ajs.282.4.451
- Blair, N. E., and R. C. Aller (2012). The fate of terrestrial organic carbon in the marine environment. *Annu Rev Mar Sci* **4**, 401-423, doi:10.1146/annurev-marine-120709-142717
- Blair, N. E., E. L. Leithold, S. T. Ford, K. A. Peeler, J. C. Holmes, and D. W. Perkey (2003). The persistence of memory: The fate of ancient sedimentary organic carbon in a modern sedimentary system. *Geochim Cosmochim Acta* **67**, 63-73, doi:10.1016/S0016-7037(02)01043-8
- Bouchez, J., O. Beyssac, V. Galy, J. Gaillardet, C. France-Lanord, L. Maurice, and P. Moreira-Turcq (2010). Oxidation of petrogenic organic carbon in the Amazon floodplain as a source of atmospheric CO₂. *Geology* **38**, 255-258, doi:10.1130/G30608.1

- Brodie, C. R., J. S. L. Casford, J. M. Lloyd, M. J. Leng, T. H. E. Heaton, C. P. Kendrick, and Z. Yongqiang (2011). Evidence for bias in C/N, $\delta^{13}\text{C}$ and $\delta^{15}\text{N}$ values of bulk organic matter, and on environmental interpretation, from a lake sedimentary sequence by pre-analysis acid treatment methods. *Quat Sci Rev* **30**, 3076-3087, doi:10.1016/j.quascirev.2011.07.003
- Carey, A. E., C. B. Gardner, S. T. Goldsmith, W. B. Lyons, and D. M. Hicks (2005). Organic carbon yields from small, mountainous rivers, New Zealand. *Geophys Res Lett* **31**, L15404, doi:10.1029/2005GL023159
- Dijkstra, P., A. Ishizu, R. Doucett, S. C. Hart, E. Schwartz, O. V. Menyailo, and B. A. Hungate (2008). ^{13}C and ^{15}N natural abundance of the soil microbial biomass. *Soil Biol Biochem* **38**, 3257-3266, doi:10.1016/j.soilbio.2006.04.005
- France-Lanord, C., and L. A. Derry (1994). $\delta^{13}\text{C}$ of organic carbon in the Bengal Fan: Source evolution and transport of C₃ and C₄ plant carbon to marine sediments. *Geochim Cosmochim Acta* **58**, 4809-4814, doi:10.1016/0016-7037(94)90210-0
- France-Lanord, C. and L. A. Derry (1997). Organic carbon burial forcing of the carbon cycle from Himalayan erosion. *Nature* **390**, 65-67, doi:10.1038/36324
- Galy, V., J. Bouchez, and C. France-Lanord (2007a). Determination of total organic carbon content and $\delta^{13}\text{C}$ in carbonate-rich detrital sediments. *Geostand Geoanal Res* **31**, 199-207, doi:10.1111/j.1751-908X.2007.00864.x

Galy, V., C. France-Lanord, O. Beyssac, P. Faure, H. Kudrass, and F. Palhol (2007b). Efficient organic carbon burial in the Bengal fan sustained by the Himalayan erosional system. *Nature* **450**, 407-410, doi:10.1038/nature06273

Gomez, B., W. T. Baisden, and K. M. Rogers (2010). Variable composition of particle-bound organic carbon in steep-land river systems. *J Geophys Res* **115**, F04006, doi:10.1029/2010JF001713

Gordon, E. S., and M. A. Goñi (2003). Sources and distribution of terrigenous organic matter delivered by the Atchafalaya River to sediments in the northern Gulf of Mexico. *Geochim Cosmochim Acta* **67**, 2359-2375, doi:10.1016/S0016-7037(02)01412-6

Graz, Y., C. Di-Giovanni, Y. Copard, M. Elie, P. Faure, F. Laggoun Defarge, J. Lévêque, R. Michels, and J. E. Olivier (2011). Occurrence of fossil organic matter in modern environments: Optical, geochemical and isotopic evidence. *Appl Geochem* **26**, 1302-1314, doi:10.1016/j.apgeochem.2011.05.004

Hagedorn, F., P. Schleppi, P. A. Waldner, and H. Flühler (2000). Export of dissolved organic carbon and nitrogen from Gleysol dominated catchments – The significance of water flow paths. *Biogeochemistry* **50**, 137-161, doi:10.1023/A:1006398105953

Hagedorn, F., J. B. Bucher, and P. Schleppi (2001). Contrasting dynamics of dissolved inorganic and organic nitrogen in soil and surface waters of forested

catchments with Gleysols. *Geoderma* **100**, 173-192, doi:10.1016/S0016-7061(00)00085-9

Hatten, J. A., M. A. Goñi, and R. A. Wheatcroft (2012). Chemical characteristics of particulate organic matter from a small, mountainous river system in the Oregon Coast Range. *Biogeochemistry* **107**, 43-66, doi:10.1007/s10533-010-9529-z

Hegg, C., B. W. McArdell, and A. Badoux (2006). One hundred years of mountain hydrology in Switzerland by the WSL. *Hydrol Process* **20**, 371-376, doi:10.1002/hyp.6055

Hilton, R. G., A. Galy, and N. Hovius (2008a). Riverine particulate organic carbon from an active mountain belt: Importance of landslides. *Glob Biogeochem Cycles* **22**, GB1017, doi:10.1029/2006GB002905

Hilton, R. G., A. Galy, N. Hovius, M.-C. Chen, M.-J. Horng, and H. Chen (2008b). Tropical-cyclone-driven erosion of the terrestrial biosphere from mountains. *Nat Geosci* **1**, 759-762, doi:10.1038/ngeo333

Hilton, R. G., A. Galy, N. Hovius, M.-J. Horng, and H. Chen (2010). The isotopic composition of particulate organic carbon in mountain rivers of Taiwan. *Geochim Cosmochim Acta* **74**, 3164-3181, doi:10.1016/j.gca.2010.03.004

Hilton, R. G., A. Galy, N. Hovius, S.-J. Kao, M.-J. Horng, and H. Chen (2012). Climatic and geomorphic controls on the erosion of terrestrial biomass from

subtropical mountain forest. *Glob Biogeochem Cycles* **26**, GB3014,
doi:10.1029/2012GB004314

Horton, R. E. (1945). Erosional development of streams and their drainage basins; hydrophysical approach to quantitative morphology. *Geol Soc Am Bull* **56**, 275-370,
doi:10.1130/0016-7606(1945)56[275:EDOSAT]2.0.CO;2

Kao, S.-J., and K.-K. Liu (1996). Particulate organic carbon export from a subtropical mountainous river (Lanyang Hsi) in Taiwan. *Limnol Oceanogr* **41**, 1749-1757

Komada, T., E. R. M. Druffel, and S. E. Trumbore (2004). Oceanic export of relict carbon by small mountainous rivers. *Geophys Res Lett* **31**, L07504,
doi:10.1029/2004GL019512

Komada, T., E. R. M. Druffel, and J. Hwang (2005). Sedimentary rocks as sources of ancient organic carbon to the ocean: An investigation through $\Delta^{14}\text{C}$ and $\delta^{13}\text{C}$ signatures of organic compound classes. *Glob Biogeochem Cycles* **19**, GB2017,
doi:10.1029/2004GB002347

Leithold, E. L., N. E Blair, and D. W. Perkey (2006). Geomorphologic controls on the age of particulate organic carbon from small mountainous and upland rivers. *Glob Biogeochem Cycles* **20**, GB3022, doi:10.1029/2005GB002677

Lyons, W. B., C. A. Nezat, A. E. Carey, and D. M. Hicks (2002). Organic carbon fluxes to the ocean from high-standing islands. *Geology* **30**, 443-446, doi:10.1130/0091-7613(2002)030<0443:OCFTTO>2.0.CO;2

Mace, G., H. Masundire, and J. Baillie (2005). Biodiversity, in *Ecosystems and Human Well-being: Current State and Trends, Volume 1 (Millennium Ecosystem Assessment Report)*, edited by Hassan, R., R. Scholes, and N. Ash, pp. 77-122, Island Press, USA

Masiello, C. A., and E. R. M. Druffel (2001). Carbon isotope geochemistry of the Santa Clara River. *Glob Biogeochem Cycles* **15**, 407-416, doi:10.1029/2000GB001290

Meybeck, M. (1993). Riverine transport of atmospheric carbon: Sources, global typology and budget. *Water Air Soil Poll* **70**, 443-463, doi:10.1007/BF01105015

Milliman, J. D., and J. P. M. Syvitski (1992). Geomorphic/tectonic control of sediment discharge to the ocean: the importance of small mountainous rivers. *J Geol* **100**, 525-544

Nash, D. B. (1994). Effective sediment-transporting discharge from magnitude-frequency analysis. *J Geol* **102**, 79-95

Olson, D. M, E. Dinerstein, E. D. Wikramanayake, N. D. Burgess, G. V. N. Powell, E. C. Underwood, J. A. D'amico, I. Itoua, H. E. Strand, J. C. Morrison, C. J. Loucks,

T. F. Allnutt, T. H. Ricketts, Y. Kura, J. F. Lamoreux, W. W. Wettengel, P. Hedao, and K. R. Kassem (2001). Terrestrial ecoregions of the world: a new map of life on Earth. *BioScience* **51**, 933-938, doi:10.1641/00063568(2001)051[0933:TEOTWA]2.0.CO;2

Prahl, F. G., J. R. Ertel, M. A. Goñi, M. A. Sparrow, and B. Eversmeyer (1994). Terrestrial organic carbon contributions to sediments on the Washington margin. *Geochim Cosmochim Acta* **58**, 3035-3048, doi:10.1016/0016-7037(94)90177-5

Rickenmann, D. and B. McArdell (2007). Continuous measurement of sediment transport in the Erlenbach stream using piezoelectric bedload impact sensors. *Earth Surf Proc Land* **32**, 1362-1378, doi:10.1002/esp.1478

Rickenmann, D., J. M. Turowski, B. Fritschi, A. Klaiber, and A. Ludwig (2012). Bedload transport measurements at the Erlenbach stream with geophones and automated basket samplers. *Earth Surf Proc Land* **37**, 1000-1011, doi:10.1002/esp.3225

Schleppi, P., N. Muller, H. Feyen, A. Papritz, J. B. Bucher, and H. Flühler (1998). Nitrogen budgets of two small experimental forested catchments at Alptal, Switzerland. *Forest Ecol Manag* **101**, 177-185, doi:10.1016/S0378-1127(97)00134-5

Schleppi, P., N. Muller, P. J. Edwards, and J. B. Bucher (1999). Three years of increased nitrogen deposition do not affect the vegetation of a montane forest ecosystem. *Phyton* **39**, 197-204

Schleppi, P., Hagedorn, F., and I. Providoli (2004). Nitrate leaching from a mountain forest ecosystem with gleysols subjected to experimentally increased N deposition. *Water, Air and Soil Pollution: Focus* **4**, 453-467, doi:10.1023/B:WAFO.0000028371.72044.fb

Schleppi, P., P. A. Waldner, and B. Fritschi (2006). Accuracy and precision of different sampling strategies and flux integration methods for runoff water: Comparisons based on measurements of the electrical conductivity. *Hydrol Proc* **20**, 395-410, doi:10.1002/hyp.6057

Schuerch, P., A. L. Densmore, B. W. McArdeell, and P. Molnar (2006). The influence of landsliding on sediment supply and channel change in a steep mountain catchment. *Geomorphology* **78**, 222-235, doi:10.1016/j.geomorph.2006.01.025

Turowski, J. M, E. M. Yager, A. Badoux, D. Rickenmann, and P. Molnar (2009). The impact of exceptional events on erosion, bedload transport and channel stability in a step-pool channel. *Earth Surf Proc Land* **34**, 1661-1673, doi:10.1002/esp.1855

Turowski, J.M., D. Rickenmann and S.J. Dadson (2010). The partitioning of the total sediment load of a river into suspended load and bedload: a review of empirical data. *Sedimentology* **57**, 1126-1146, doi:10.1111/j.1365-3091.2009.01140.x

Turowski, J. M., A. Badoux, and D. Rickenmann (2011). Start and end of bedload transport in gravel-bed streams. *Geophys Res Lett* **38**, L04401, doi:10.1029/2010GL046558

West, A. J., C.-W. Lin, T.-C. Lin, R. G. Hilton, S.-H. Liu, C.-T. Chang, K.-C. Lin, A. Galy, R. B. Sparkes, and N. Hovius (2011). Mobilization and transport of coarse woody debris to the oceans triggered by an extreme tropical storm. *Limnol Oceanogr* **56**, 77-85, doi:10.4319/lo.2011.56.1.0077

Wheatcroft, R. A., M. A. Goñi, J. A. Hatten, G. B. Pasternack, and J. A. Warrick (2010). The role of effective discharge in the ocean delivery of particulate organic carbon by small, mountainous river systems. *Limnol Oceanogr* **55**, 161-171, doi:10.4319/lo.2010.55.1.0161

Winkler, W., W. Wildi, J. van Stuijvenberg, and C. Caron (1985). Wägital-Flysch et autres flyschs penniques en Suisse Centrale: Stratigraphie, sédimentologie et comparaisons. *Eclogae Geol Helv* **78**, 1-22

Wright, R. F., and L. Rasmussen (1998). Introduction to the NITREX and EXMAN projects. *Forest Ecol Manag* **101**, 1-7, doi:10.1016/S0378-1127(97)00120-5

Figure Captions

Figure 1. Hydrographs for 3 of the 5 storm events sampled in July 2010. Dark grey area is precipitation ($\times 100$, in mm); light grey area is discharge (Q , in l s^{-1}). Suspended sediment concentration (SSC, $\times 100$, in g l^{-1}), organic carbon concentration (C_{org} , in %), carbon isotopic composition ($\delta^{13}\text{C}$ in ‰), and organic carbon to nitrogen ratio (C/N) are represented by circles, squares, triangles, and diamonds, respectively. Final panel shows the average annual hydrograph over the 29-year monitoring period (1983-2011), and mean suspended sediment concentrations of samples collected every 1-2 weeks over a 6-year period (2005-2010) (SSC data from the Swiss National River Monitoring and Survey Programme, http://www.eawag.ch/forschung/wut/schwerpunkte/chemievonwasserressourcen/naduf/datendownload_EN).

Figure 2. Variation of organic carbon concentration in riverine suspended sediment with total suspended load (note logarithmic x -axis). Open symbols are background flow ($Q/Q_{\text{mean}} < 10$). POC = particulate organic carbon.

Figure 3. Top: nitrogen to carbon ratios (N/C) and carbon isotopic composition ($\delta^{13}\text{C}$) of Erlenbach riverine suspended sediment, hillslope runoff suspended sediment and major stores of carbon within the catchment. Bottom: carbon to nitrogen ratios (C/N) and nitrogen isotopic composition ($\delta^{15}\text{N}$) of the same pools.

Figure 4. Zoomed-in views of the plots in Figure 3, where suspended sediment samples are colour-coded according to total suspended load (warm colours represent

low values; cold colours represent high values). Open squares are background flow ($Q/Q_{\text{mean}} < 10$). 'Fossil end member' includes bedrock, bedload, channel banks and landslides. Dotted lines indicate potential mixing zones between the fossil end member and non-fossil sources. Determination and nature of the hypothetical non-fossil end member is discussed section 5.1.

Figure 5. Rating curves showing power law relationships between Q/Q_{mean} and suspended sediment concentration, total POC (tPOC), fossil POC (fPOC) and non-fossil POC (nfPOC), all in mg l^{-1} . POC is particulate organic carbon concentration. Small squares represent individual samples; open symbols are background flow ($Q/Q_{\text{mean}} < 10$). Dashed lines are 95% confidence bands.

Table 1. Characteristics of the five storm events sampled.

Date	Approx. time (UTC+2)	Number of samples^a	Peak Q (l s⁻¹)	Peak Q/Q_{mean}^b
12 July 2010	19.00-20.30	37	2290	59
22-23 July 2010	20.30-02.30	37 + 1 preceding	420	11
26 July 2010	21.00-00.00	16 + 1 preceding	300	8
29 July 2010	06.30-16.45	25	1190	31
30 July 2010	08.45-16.00	9	1580	41

^aAdditional samples for 22 and 26 July were collected at intervening low flow.

^bQ/Q_{mean} is the discharge relative to the average discharge over the period 1983-2011 inclusive (38.6 l s⁻¹).

Table 2. Organic carbon concentration (C_{org}), carbon to nitrogen ratio (C/N), carbon isotopic composition ($\delta^{13}C$) and nitrogen isotopic composition ($\delta^{15}N$) of major carbon stores within the catchment, and hillslope runoff and riverine suspended sediment^a.

	<i>n</i>	C_{org} (%)		C/N		$\delta^{13}C$ (‰)		$\delta^{15}N$ (‰)	
		Mean	σ	Mean	σ	Mean	σ	Mean	σ
Bedrock	22	0.54 ± 0.11	0.26	7.81 ± 1.7	3.98	-25.71 ± 0.36	0.84	3.34 ± 0.26	0.60
Bedload	11	0.87 ± 0.21	0.36	9.78 ± 0.9	1.57	-25.84 ± 0.10	0.17	2.13 ± 0.23	0.38
Channel banks	8	0.87 ± 0.22	0.32	8.12 ± 1.1	1.58	-25.89 ± 0.40	0.57	2.91 ± 0.29	0.40
Landslide profile	22	0.64 ± 0.06	0.15	7.38 ± 0.4	0.87	-26.03 ± 0.12	0.28	2.67 ± 0.30	0.71
Deep soil ^b	10	2.15 ± 1.2	1.85	11.8 ± 2.3	3.64	-25.98 ± 0.34	0.54	3.56 ± 1.99	3.14
Surface soil ^b	17	16.5 ± 6.3	12.9	17.9 ± 2.2	4.45	-26.84 ± 0.48	0.98	-1.33 ± 0.77	1.59
Foliage	8	46.9 ± 2.0	2.88	55.5 ± 17	24.2	-28.30 ± 1.13	1.60	-5.87 ± 1.67	2.36
Woody debris	12	49.1 ± 1.8	3.18	173 ± 98	170	-25.25 ± 0.69	1.19	-3.99 ± 1.29	2.24
<i>Hypothetical non-fossil end member</i>	-	-	-	15.8 ± 6.8	-	-27.15 ± 0.53	-	0.61 ± 1.40	-
Forest hillslope runoff	38	9.12 ± 0.9	2.77	12.6 ± 0.7	2.28	-26.50 ± 0.08	0.23	2.48 ± 0.30	0.93
Meadow hillslope runoff	10	15.9 ± 1.7	2.67	12.6 ± 1.8	2.91	-26.56 ± 0.50	0.79	4.43 ± 1.04	1.64
Riverine suspended sediment ^c	122	1.45 ± 0.06	0.32	9.55 ± 0.2	1.34	-26.33 ± 0.08	0.45	2.21 ± 0.16	0.87
<i>Rising limb</i>	72	1.36 ± 0.07	0.29	9.89 ± 0.3	1.35	-26.45 ± 0.08	0.32	1.95 ± 0.13	0.56
<i>Falling limb</i>	50	1.57 ± 0.09	0.33	9.16 ± 0.4	1.29	-26.16 ± 0.15	0.54	2.58 ± 0.31	1.09
<i>Raining</i>	85	1.40 ± 0.06	0.29	10.0 ± 0.3	1.32	-26.49 ± 0.07	0.34	1.94 ± 0.12	0.53
<i>Dry</i>	37	1.55 ± 0.12	0.37	8.69 ± 0.4	1.07	-25.98 ± 0.15	0.47	2.83 ± 0.38	1.15

^a σ = standard

deviation; errors are ± twice the standard error on the mean.

^bSurface soil samples were collected from the top ~10cm (without overlying vegetation); deep soil samples were collected from below 10 cm in two vertical profiles.

^cRiverine suspended sediment is subdivided into samples collected during i) rising and falling limbs and ii) active rainfall and dry periods.

Table 3. Results of radiocarbon analysis on selected samples^a.

Sample Type	Q (l s ⁻¹)	Sample ID	Publication code	C _{org} (%)	F _{mod} (fraction of modern C) ^b	Δ ¹⁴ C (‰)	Conventional radiocarbon age (years BP)
Suspended sediment	78	12.7 1748	SUERC-40494	2.2	0.68 ± 0.004	-317.9 ± 3.5	3073 ± 41
	394	12.7 1719	SUERC-39226	1.2	0.67 ± 0.003	-328.0 ± 3.2	3193 ± 38
	517	29.7 1768	SUERC-39232	1.3	0.47 ± 0.002	-530.5 ± 2.3	6074 ± 39
	1170	12.7 1711	SUERC-39229	2.2	0.74 ± 0.004	-256.5 ± 3.5	2381 ± 38
	2060	12.7 1707	SUERC-39230	1.9	0.69 ± 0.003	-314.4 ± 3.2	3033 ± 38
	2290	12.7 1729	SUERC-39231	1.8	0.67 ± 0.003	-333.8 ± 3.2	3262 ± 38
Surface soil		ER-ST-1-L-0	SUERC-39216	1.2	0.53 ± 0.003	-471.7 ± 2.6	5123 ± 39
		ER-ST-2-L-15	SUERC-39219	6.0	1.00 ± 0.005	-3.5 ± 4.7	Modern
		ER-ST-1-R-350	SUERC-39220	25	1.06 ± 0.005	64.8 ± 5.0	Modern
		ER-ST-1-R-20	SUERC-39221	11	1.05 ± 0.005	53.9 ± 5.0	Modern
Wood entrained in bedload		ER-V-19	SUERC-39222	50	0.81 ± 0.004	-186.5 ± 3.8	1658 ± 37
		ER-V-11	SUERC-39223	50	1.00 ± 0.005	-0.1 ± 4.5	Modern
Wood entrained in landslides		ER-V-17	SUERC-39224	52	0.87 ± 0.004	-132.1 ± 4.1	1138 ± 38
		ER-V-20	SUERC-39225	50	0.61 ± 0.003	-392.9 ± 2.7	4009 ± 36

^aErrors are ±1σ.

^bReference date for F_{mod} is 1950; therefore F_{mod} can be >1 in plants and soils due to incorporation of ¹⁴C from nuclear weapons testing during the second half of the twentieth century.

Table 4. Rating curve parameters for power law relationships between Q/Q_{mean} and suspended sediment (SS) or particulate organic carbon (POC), of the form $SS \text{ or POC} = a(Q/Q_{\text{mean}})^{b(a)}$.

	<i>a</i>	<i>b</i>	$R^{2(b)}$	$Q_e \text{ (l s}^{-1}\text{)}^c$	$Q_e \text{ (}Q/Q_{\text{mean}}\text{)}^c$
SS	99.7 ± 29.4	1.19 ± 0.08	0.78	300	7.7
	<i>96.0 ± 44.2</i>	<i>1.20 ± 0.12</i>	<i>0.68</i>		
tPOC	0.96 ± 0.30	1.33 ± 0.08	0.81	400	10.4
	<i>0.96 ± 0.48</i>	<i>1.33 ± 0.13</i>	<i>0.71</i>		
fPOC	0.80 ± 0.39	1.08 ± 0.13	0.50	230	5.6
	<i>0.75 ± 0.64</i>	<i>1.10 ± 0.23</i>	<i>0.32</i>		
nfPOC	0.41 ± 0.20	1.45 ± 0.13	0.70	520	13.4
	<i>0.44 ± 0.33</i>	<i>1.43 ± 0.20</i>	<i>0.57</i>		

^aValues in regular type (used for flux calculations) are based on the whole sample set; values in italics are based only on samples with $Q/Q_{\text{mean}} > 10$. There are three classes of POC: total (tPOC), fossil (fPOC) and non-fossil (nfPOC).

^bCorrelation coefficients are given as R^2 .

^c Q_e is the effective discharge, as defined by Wheatcroft et al. (2010). Q/Q_{mean} is the discharge relative to the average discharge over the period 1983-2011 inclusive (38.6 l s^{-1}).

Table 5. Modeled export of suspended sediment (SS) and total, fossil and non-fossil particulate organic carbon (tPOC, fPOC and nfPOC), averaged over 29 years (1983-2011 inclusive).

	Mean annual yield (tonnes)	Mean annual yield (tonnes) according to Q/Q_{mean} (l s^{-1}). Proportions in each class are given in brackets.				Export flux ($\text{t km}^{-2} \text{ yr}^{-1}$)
		$Q/Q_{\text{mean}} \leq 1$ (77%)	$1 < Q/Q_{\text{mean}} \leq 10$ (22%)	$10 < Q/Q_{\text{mean}} \leq 60$ (1%)	$Q/Q_{\text{mean}} > 60^b$ (<0.01%)	
SS	1220 ± 232	12.0 ± 0.79 (1.1%)	376 ± 35.3 (32%)	740 ± 91.8 (61%)	91.1 ± 61.3 (5.8%) <i>215 ± 171 (10%)</i>	1648 ± 313
tPOC	17.3 ± 4.3	0.11 ± 0.01 (0.7%)	4.57 ± 0.44 (28%)	11.0 ± 1.40 (64%)	1.57 ± 1.06 (6.9%) <i>4.21 ± 3.43 (12%)</i>	23.3 ± 5.8
fPOC	7.44 ± 1.2	0.10 ± 0.01 (1.5%)	2.56 ± 0.24 (36%)	4.30 ± 0.53 (58%)	0.47 ± 0.32 (5.1%) <i>1.02 ± 0.79 (8.6%)</i>	10.1 ± 1.6
nfPOC	10.4 ± 3.2	0.04 ± 0.00 (0.5%)	2.39 ± 0.23 (26%)	6.85 ± 0.88 (67%)	1.10 ± 0.74 (7.3%) <i>3.29 ± 2.73 (13%)</i>	14.0 ± 4.4
F_{nf}^a	0.61 ± 0.02	0.30 ± 0.00	0.48 ± 0.00	0.61 ± 0.00	0.70 ± 0.00 <i>0.76 ± 0.02</i>	-

^a F_{nf} is the modeled fraction of organic carbon derived from non-fossil sources, given overall in the first column and then for separate discharge classes.

^bFor $Q/Q_{\text{mean}} > 60$, the top line (normal type; used in calculating overall yields and fluxes) assumes that the rating curves are flat from $Q/Q_{\text{mean}} = 60$; the bottom line (italics; given for comparison only) assumes that the same rating relationships apply above this limit.

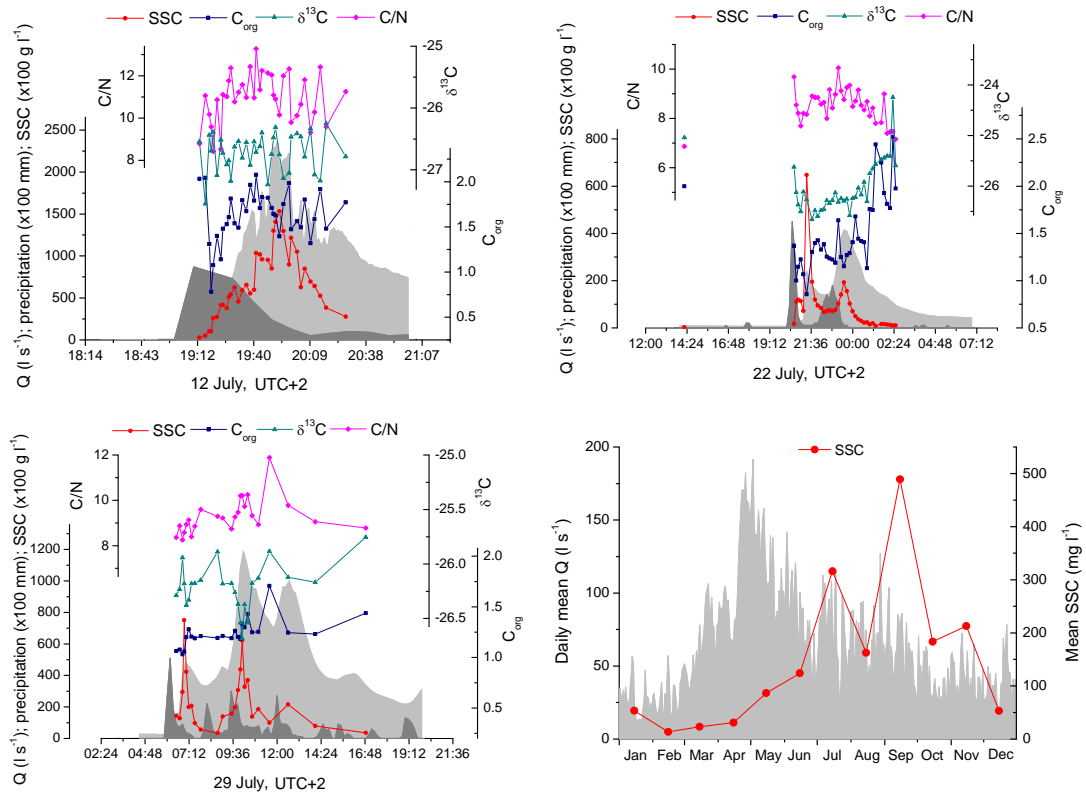


Figure 1

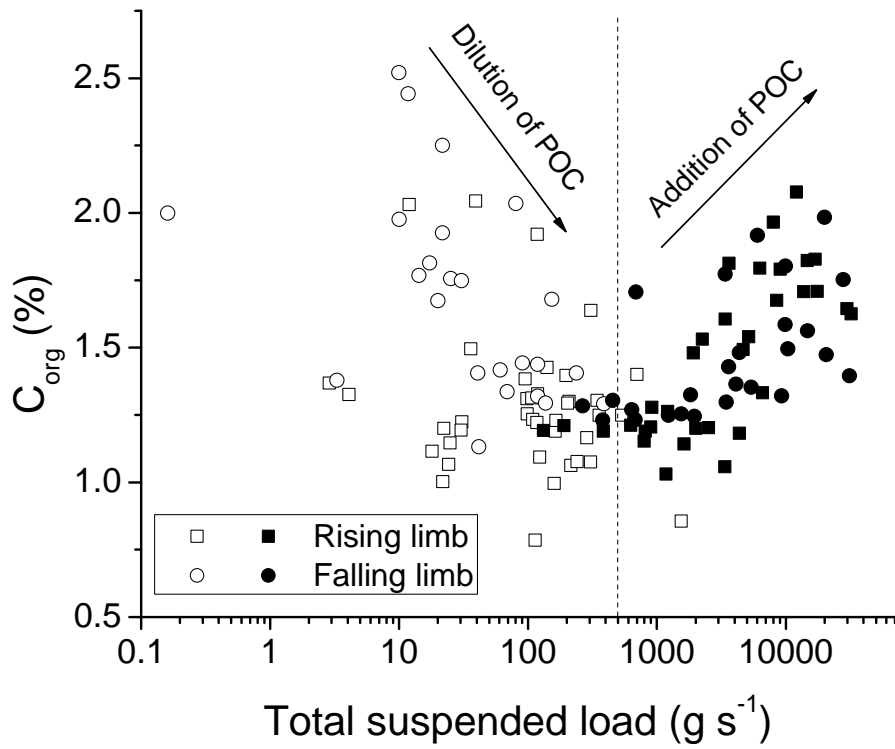


Figure 2

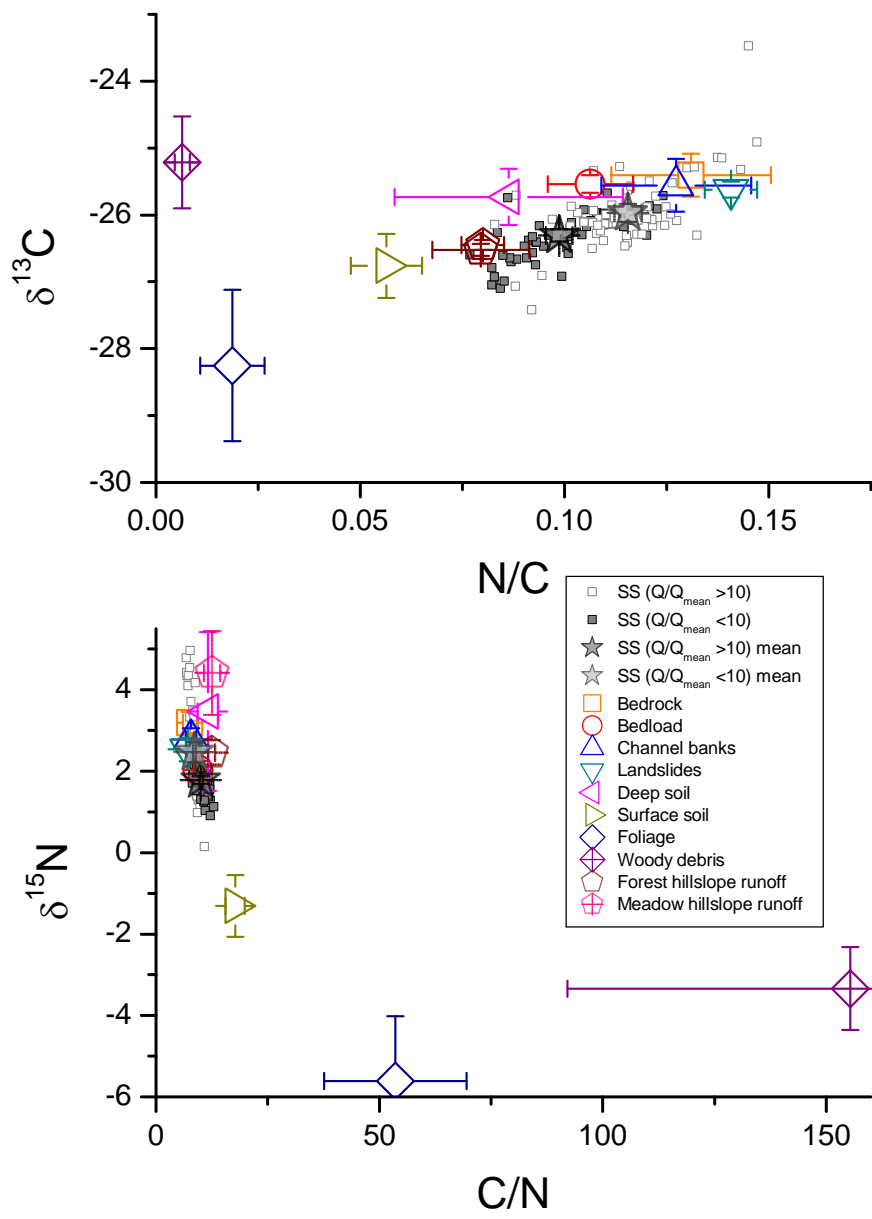


Figure 3

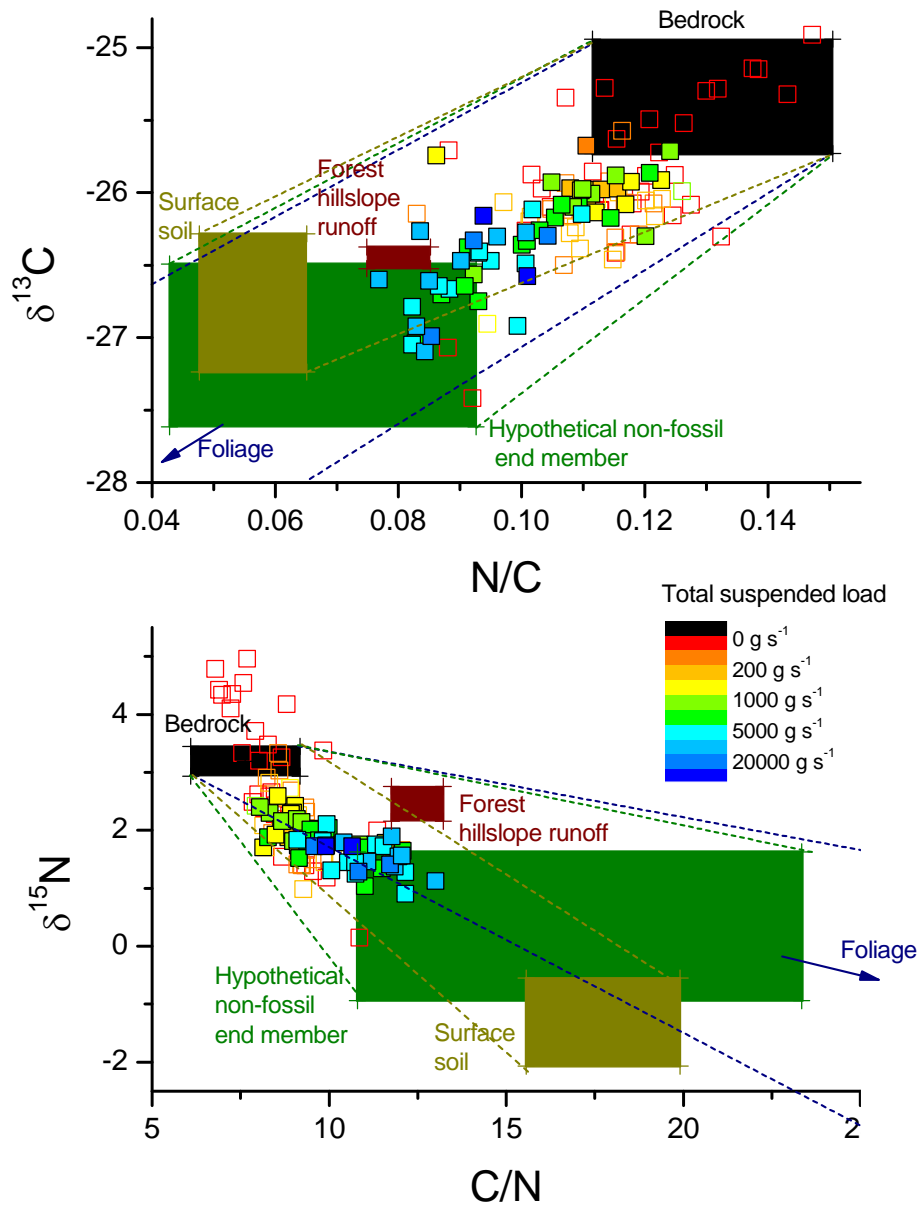


Figure 4

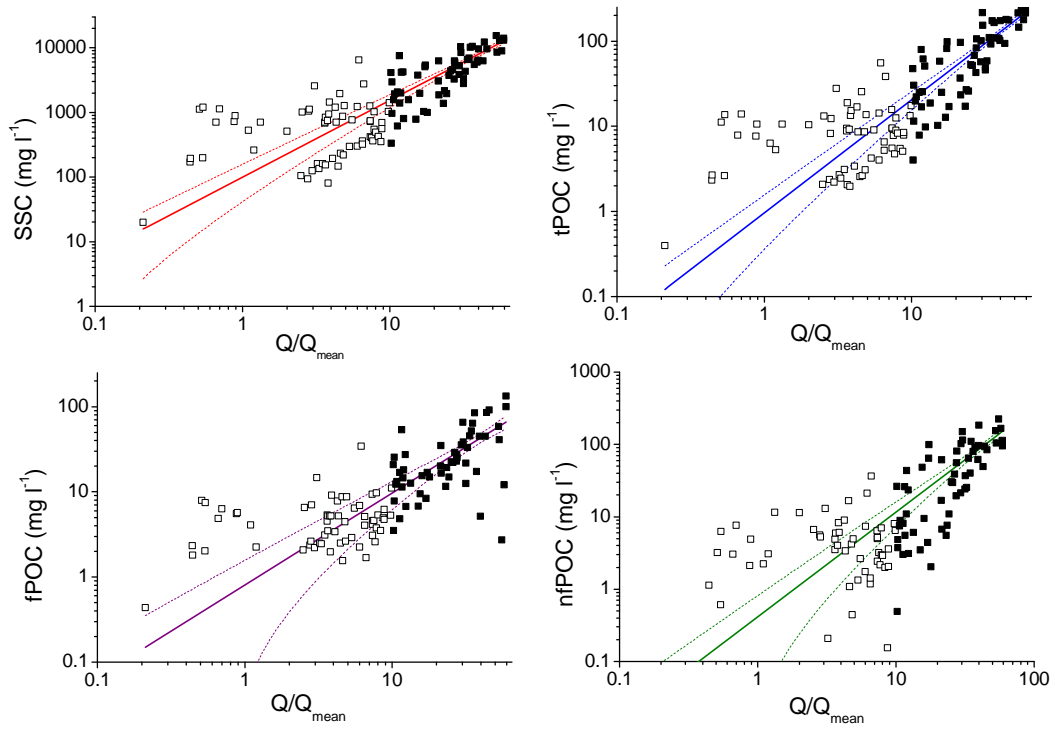


Figure 5